Published in final edited form as:
*Adv Funct Mater*. 2010 November 9; 20(21): 3721–3726. doi:10.1002/adfm.201000711.

# Stable Encapsulation of QD Barcodes with Silica Shells**

**Mr Shang-Hsiu Hu**[§] and **Prof. Xiaohu Gao**[*,§]

Xiaohu Gao: xgao@uw.edu

[*]Department of Bioengineering, University of Washington, Seattle, WA 98195 (USA)

[§]Department of Materials Sciences and Engineering, National Chiao Tung University, Hsinchu, 300 (Taiwan)

## Abstract

Quantum dot-doped mesoporous microbeads (QDMMs) are encapsulated with silica shells for enhanced chemical stability. The results show that a micro-emulsion procedure is highly efficient in coating QDMMs with polyvinyl alcohol (PVA), which is important in the subsequent deposition of a silica shell. Incorporation of fluorescent silane precursors allows direct observation of silica shells by fluorescence microscopy. The resulting silica coated QDMMs (QDMM@$SiO_2$) exhibit remarkable stability against solvent-induced QD leaching and chemical-induced fluorescence quenching compared with uncoated QDMMs. Further development of this technology such as optimization of silica shell thickness, surface modification with non-fouling polymers, and conjugation with biomolecular probes will enable clinical translation of the optical barcoding technology for highly multiplexed detection and screening of genes and proteins.

### Keywords

mesoporous; quantum dots; barcoding; silica; encapsulation

## 1. Introduction

Optical barcoding technology based on fluorophore encoded microbeads has become an important alternative to planar chip-based assays for highly multiplexed gene and protein screening. In contrast to DNA microarrays that are spatially encoded, microbead barcodes are produced and resolved based on spectral information.[1–7] For example, we have previously reported the preparation of polystyrene microbeads encoded with multicolor QDs.[5] The use of six colors and 10 intensity levels can theoretically encode one million biomolecules. Enabled by the unique optical properties of QDs, QD-doped microbeads offer key advantages over traditional organic fluorophore labeled microspheres, such as a dramatically increased number of possible barcodes, and single light source excitation of multiple colors. Most recently, we improved the barcode fluorescence intensity and uniformity by two orders of magnitude by combining QDs with mesoporous silica and polystyrene microbeads.[8, 9] The pore sizes are typically engineered to 30–100 nm for fast QD doping and uniform QD distribution inside microbeads. A key factor contributing to the improved brightness is the large surface area (150 $m^2$ per gram of beads) of mesoporous materials, about 50–100 times larger than that of nonporous beads of the same size.

**This work was supported in part by NIH (R01 CA131797), NSF (0645080), and the Department of Bioengineering at the University of Washington. X.H.G. thanks the NSF for a Faculty Early Career Development award (CAREER). S.H.H. thanks Prof. San-Yuan Chen and the National Science Council of Taiwan for a generous study abroad fellowship. We are also grateful to UW-NTUF for SEM, and Dr. Y Andrew Wang at Oceannanotech for quantum dots.

Despite these recent achievements, a number of issues of the QD optical barcoding technology must be addressed before its clinical translations. In particular, since the microbeads are mesoporous, potential leaching and chemical-induced degradation (*e.g.*, spectral shift and intensity variation) of the embedded QDs are of major concerns. For example, when organic solvents are used to disperse microbeads, QDs slowly diffuse out of the pores resulting in a loss of barcode fluorescence intensity. Similarly, fluorescence fluctuation is often observed in different biological buffers or in reactions with bioconjugation crosslinking reagents. In addition, the mesoporous microbeads have poor water solubility because both the inner and outer surfaces of the beads are terminated with hydrocarbons. This high hydrophobicity is well suited for QD incorporation driven by multivalent hydrophobic interactions. On the other hand, it also creates two problems, low solubility of the beads in aqueous solutions and lack of functional groups for biomolecule conjugation.

To address these limitations, here, we report a simple method for encapsulation of QDMMs with silica shells to stabilize the embedded QDs. As schematically illustrated in Fig. 1, PVA was first coated onto hydrophobic QDMMs via a microemulsion process. Silica precursor, tetraethylorthosilicate (TEOS), was then hydrolyzed and deposited onto QDMM surface catalyzed by bases. The resulting QDMM@$SiO_2$ beads have a high density of hydroxyl groups on their surface for better water solubility. To functionalize the microbeads with primary amines for simple bioconjugation and direct observation of the silica coating, a mixture of TEOS and organic dye labeled aminopropyl-trimethoxysilane (APTMS) are copolymerized. Because QDs have broad absorption profiles, green-emitting organic fluorophores (FITC) and red-emitting QDs are used in the current study for simultaneous excitation of both colors with a single light source.

## 2. Results and Discussion

### 2.1 Silica encapsulation

Fig. 2 shows true color fluorescence and scanning electron microscopy (SEM) images of QDMM@$SiO_2$ in comparison with the original uncoated QDMM. The QD doped microbeads were extremely bright and appeared unchanged after silica encapsulation regardless of the excitation wavelength. Under UV illumination, QDMM fluorescence was stronger than that under blue light excitation because the embedded QDs have increasing molar absorption coefficient toward shorter wavelength.[10] For direct visualization of the silica shells, a fluorescent silane compound was included as one of the reactants. APTMS-FITC was prepared by mixing APTMS and FITC in ethanol. The condensation reaction between the primary amine in APTMS and the isothiocyanate group in FITC in ethanol is highly efficient. Indeed, this reaction has been used to monitor the accessibility of amino groups in postsynthetically functionalized mesoporous silica.[11, 12] The molar ratio of TEOS, APTMS, and APTMS-FITC was set at approximately 100:10:1. APTMS-FITC provides a fluorescent signal for microscopic examination of the silica shells, whereas APTMS has primary amine groups for potential crosslinking reactions with biomolecules. When excited at 350 nm, only red QDs were visible under fluorescence microscope. In contrast, due to the broad absorption spectra of QDs, excitation at longer wavelength (around 480 nm) enabled simultaneous detection of both red QDs and green FITC molecules, revealing the formation of silica shells. As a result, switching between the two excitation wavelengths becomes a simple method to distinguish QDMM@$SiO_2$ from QDMM when the two types of microbeads are mix together, an assay utilized for microbead stability comparisons discussed below.

Under the current fluorescence imaging conditions, it is difficult to determine the silica shell thickness or the penetration depth of the silica shell into the mesopores. It is unlikely,

however, that the newly formed silica completely fills the microbeads' pores. Several lines of evidence support this hypothesis. First, some of the microbeads clearly exhibit a ring structure on their surface indicating the presence of a shell structure. Second, the silica precursors have high water solubility, which limits their penetration into the highly hydrophobic pores. Third, if silica completely infiltrates the pores and interacts with embedded QDs, a significant decrease in fluorescence would be observed. For example, it has been shown in silica encapsulation of single QDs that the QD fluorescence is reduced by 60–90% due to surface ligand exchange.[13] To determine the exact penetration depth of the silica shell, however, the microbeads will need to be cut into thin sections.[8]

We further examined the surface properties of the microbeads with SEM as shown in Fig. 2g to 2l. QDMMs appear relatively smooth on the outer surface despite the large pores. After coating with silica shells, the surface of QDMMs became rough and granular likely due to some small silica nanoparticles attached to the microbead surface. However, no crevices or cracks were detected, indicating the formation of complete silica shells. Due to the broad size variation of the original silica microbeads, the size increase after silica shell formation was difficult to estimate. This problem could be solved by using more uniform mesoporous microbeads such as polystyrene microbeads.[9]

It is worth mentioning that under the current experiment conditions, PVA plays a pivotal role in silica shell formation. Without it, the incompatibility between the hydrophobic hydrocarbons on microbead surface and hydrophilic silane compounds hinders nucleation of silane onto microbead surface. To stabilize the hydrophobic microspheres in polar solvents and create anchor points for silane condensation, a number of amphiphilic non-ionic polymers (*e.g.*, polyvinylpyrrolidone or PVP,[14, 15] PVA,[16] and hydroxypropyl cellulose or HPC[17, 18]) have been proven effective, offering important advantages over simple surfactant molecules. Unlike small-molecule surfactants, these polymers do not have long-chain hydrocarbons that can interdigitate with QDs' surface ligands and consequently solubilize QDs (resulting in QD leaching). Based on our prior experience,[16] we proceeded with PVA to stabilize the microbeads. Our initial attempt by mixing QDMMs and PVA in aqueous solution, however, was not successful. Fig. 3 shows that after addition of silane compounds, they did not nucleate on the surface of QDMMs and further develop into shells; instead, they self-nucleated in solution and condensed into irregularly shaped aggregates. This is likely due to poor coverage of PVA on QDMMs. We solved this problem by employing a microemulsion procedure that drives PVA onto microbead surface. The microbeads were initially suspended in organic solvents and PVA was used as a polymer surfactant that stabilizes oil droplets in aqueous solution. As the organic phase evaporated, PVA at the boundary of organic and water phase attached to the microbeads and served as anchor points for silica deposition (Fig. 2 a–f).

### 2.2 Physical and chemical stability of the embedded QDs

Despite the high brightness of QDMMs, a major concern was leaching of the doped QDs if the mesopores were not sealed. We have previously shown that embedded QDs do not diffuse out of the microbeads in polar solvents such as water and ethanol.[8] This is not surprising since tri-n-octylphosphine oxide (TOPO) coated QDs have extremely low solubility in these solvents. However, when organic solvents such as toluene, chloroform, butanol or their mixtures are used, doped QDs quickly partition back into the solution phase, significantly altering the original optical barcodes. As shown in Fig. 4b, after QDMMs were suspended in mixture solvent of chloroform and butanol (v/v 9:1) and free QDs were removed by centrifugation, the QDMMs became nearly non-fluorescent. Note that addition of 10% butanol is to ensure dispersity of QDMM@$SiO_2$ in the following study because the hydrophilic QDMM@$SiO_2$ are not soluble in pure chloroform. Quantitative spectroscopic measurements confirmed that greater than 85% of the embedded QDs leached out of the

microbeads (Fig. 4c). In contrast, both fluorescence imaging and spectroscopy show that the fluorescence of QDMM@$SiO_2$ remained nearly identical after chloroform treatment (Fig. 4d–f). This result clearly indicates that the $SiO_2$ layer acts as an effective barrier to block QDs from dissolving into solvents.

To compare the chemical stability of the QDMMs before and after silica shell coating, the microbeads were challenged for 24 hours with aqueous solutions of various pH and chemical crosslinkers often used in bioconjugation. As shown in Fig. 5, QDMMs with unsealed pores are highly sensitive to the environment. When the microbeads were suspended in aqueous solutions with pH values ranging from 1 to 12 (fluorescence at neutral pH was set to 100%), small changes in pH resulted in significant fluorescence fluctuation. For example, reducing pH from 7 to 5–6, a condition often used in carbodiimide based acid-amine condensation, the fluorescence of embedded QDs was reduced by more than 50%. When the pH value was increased by 1 (to pH 8), the fluorescence signal enhanced by approximately 20%. Similar effect has been observed by us and others on single QDs,[19–22] and this pH dependent fluorescence enhancement has been attributed to better passivation of surface traps by hydroxides.[21] In contrast, change of QDMM@$SiO_2$ fluorescence was negligible in solutions of pH 5–8, the most common pH range used in bioconjugation and molecular detection experiments. As the pH value increased above 9, the fluorescence from QDMM@$SiO_2$ also slowly increased, likely due to degradation of the $SiO_2$ layer because silica is not stable in strong base. Under strong acidic conditions (not encountered in most biological assays though), the fluorescence of QDMM@$SiO_2$ gradually decreased, although at a slower rate than the unprotected QDMMs, suggesting that the thin silica shells are not acid impermeable. This problem could be solved by coating thicker layers of silica onto microbead surfaces. To further characterize the kinetics of acid quenching, we imaged the QDMMs with and without silica protection in real time (Fig. 5b). QDMM and QDMM@$SiO_2$ mixture were treated with pH 4 solution followed by fluorescence microscopy examination. The two sets of microbeads were easily distinguishable when excited at 480 nm because the QDMM@$SiO_2$ labeled with FITC exhibited a green circle on the microbead surface but not the unprotected QDMMs. Continuous incubation led to significant spectral shift toward shorter wavelength for the unprotected microbeads (emission changed from red to green), indicating degradation or partial dissolving of the initial red QDs.[22] Within 40 seconds of incubation, the quenched QDs became difficult to detect. In contrast, the QDMM@$SiO_2$ remained highly fluorescent during the same incubation period.

Next, we probed the stability of QDMMs against chemical treatments, with a focus on compounds frequently used in bioconjugation reactions. This is an important test because the QD doped microbeads have no specificity toward any gene or protein targets and thus must be functionalized with biomolecular probes such as oligonucleotides, peptides, or antibodies. Fig. 5c shows that the QDMM@$SiO_2$ is significantly more stable than the unprotected QDMM. When crosslinking reagents such as 1-ethyl-3-(3-dimethylaminopropyl) carbodiimide (EDC), N-hydroxysuccinimide (NHS), and Sulfosuccinimidyl 4-N-maleimidomethyl cyclohexane-1-carboxylate (SMCC) were added, the QDMM fluorescence decreased up to approximately 90% after 24 hour incubation. In contrast, QDMM@$SiO_2$ fluorescence was nearly unaffected under the same condition. We note that the $SiO_2$ shell at current thickness does not shield the embedded QDs completely from the environment. For example, N-e-Maleimidocaproic acid (EMCA) could quench the fluorescence of QDs in QDMM@$SiO_2$ by 20%. Again, this problem could be solved by growing a thicker silica shell or decorating additional protection layers on top of the silica shell.

## 3. Conclusions

In summary, we have developed a method to stably encapsulate QD barcodes with silica shells. To stabilize hydrophobic mesoporous microbeads in polar solvents, a microemulsion process was found highly effective in uniformly coating amphiphilic polymers onto the microbead surface. Subsequent condensation of silane compounds resulted in QDMM@$SiO_2$ with significantly improved chemical stability. This new method solved key problems in QD barcoding technology such as nanoparticle leaching. When QDMM@$SiO_2$ was suspended in organic solvents such as chloroform, in which hydrophobic QDs have excellent solubility, negligible nanoparticle leaching was detected. Furthermore, the barcode fluorescence remained stable when treated for 24 hours with pH 5–8 aqueous solutions and a variety of common bioconjugation crosslinkers. We envision that further optimization of this method such as fine tuning the silica shell thickness and linking silica surface with non-fouling polymers will allow clinical translation of the QD barcoding technology.

## 4. Experimental

### Materials and instruments

Unless specified, chemicals were purchased from Sigma-Aldrich and used without further purification. Organic soluble core-shell CdSe/ZnS quantum dots were a gift from Oceannanotech LLC. Mesoporous silica microbeads (5 μm in diameter, 32 nm pore size) with surface terminated with $C_{18}$ (octadecyl chain) were purchansed from Phenomenex (Torrance, CA). SEM images of the microbeads were obtained using a FEI Sirion XL30 Field Emission SEM (Hillsboro, OR). For SEM analysis, microbeads were dried on silicon wafers (0.5×0.5 cm) and treated with gold/platinum sputtering. The SEM operating voltage was set at 5 kV, and the working distance was about 5 mm. True-color fluorescence images was obtained on an inverted microscope (IX-71, Olympus, San Diego, CA) equipped with a digital camera (Q-color 5, Olympus) and a variety of filter sets (Chroma, Rockingham, Vt). A fluorometer (Fluoromax4, Horiba Jobin Yvon, Edison, NJ) was used to characterize the emission spectra of QD doped mesoporous silica beads.

### Doping

The protocols of QD doping into mesoporous silica beads was reported in our previous work.[8] Briefly, 0.5 ml of 4 nM QDs in chloroform was mixed one million MMs in 2 ml of butanol, yielding a doping level of approximately 1.2 million dots per beads. The doping process was complete in less than 10 min with negligible amount of free QDs left in solution. The resulting QDMMs were isolated by centrifugation and washed three times with ethanol.

### Encapsulating QDMMs with silica shells

60 mg of PVA (mw=9,000~10,000) as a polymer surfactant was dissolved in 3 ml D.I. water at 70 °C. After PVA completely dissolved, the clear solution was cooled to room temperature. The QDMMs were isolated with centrifugation (2,000 rpm for 4 minutes) and quickly redispersed in 0.5 ml chloroform. The organic phase was immediately added to the PVA solution, and the mixture was emulsified for several minutes with an ultrasonicator and a vortex. The emulsion was then stirred at room temperature for 90 minutes to evaporate the organic phase. After evaporation of organic solvent, the PVA coated QDMMs (QDMM@PVA) were washed by D.I. water for 3 times and isolated by centrifugation. The precipitated microbeads were redispersed in 3 ml of 99.5 % ethanol, followed by addition of 10 μl of tetraethylorthosilicate for $SiO_2$ shell formation. 50 μl of 33% $NH_4OH$ was slowly added to initiate silica polymerization, and the mixture was stirred for 4 hours. The resulting QDMM@$SiO_2$ were rinsed repeatedly with water and ethanol to remove excess reactants

from the silica shell formation reaction and with chloroform to remove small amount of QDs attached to the silica shell surface. For direct visualization of silica shells on QDMMs, fluorescent silane compound was used. Fluorescein isothiocyanate (FITC) was mixed with ethanolic 3-aminopropyltrimethoxysilane (APTMS) solution for 24 h at room temperature to form N-1-(3-trimethoxysilylpropyl)- N-fluoresceyl thiourea (APTMS-FITC). The molar ratio of FITC to APTMS was 1/10. To QDMM@PVA dispersed in 3 ml of 99.5 % ethanol, 45nmole of TEOS, 4.5nmole of APTMS, and 0.45 nmole APTMS-FITC were added followed by slow addition of 50 μl of 33% $NH_4OH$. The rest of the protocols are identical to the QDMM coated with non-fluorescent silica shell.

### Chemical stability of core-shell beads

Dispersions of QDMM before and after silica encapsulation were challenged with solutions of various pH values and common crosslinking reagents. For the pH study, microbeads were incubated in solutions with pH ranging between 1 and 12 for 24 hours. For chemical stability study, microbeads (0.1 wt%) were incubated with seven representative chemicals often used in bioconjugation for 24 hours at room temperature. The concentrations of the chemicals used in this study were as follow, 5 mM of EDC, 5 mM of NHS, 0.25 mM of bis(sulfosuccinimidyl) suberate ($BS_3$), 5 mM of EMCA, 0.25 mM of sulfo-SMCC, 0.05 mg/ml of Biotin, and 0.05 mg/ml of Streptavidin.

## References


1. Ferguson JA, Boles TC, Adams CP, Walt DR. Nat Biotechnol. 1996; 14:1681. [PubMed: 9634851]
2. Fulton RJ, McDade RL, Smith PL, Kienker LJ, Kettman JR Jr. Amer Assoc Clin Chem. 1997; 43:1749.
3. Battersby BJ, Bryant D, Meutermans W, Matthews D, Smythe ML, Trau M. J Am Chem Soc. 2000; 122:2138.
4. Steemers FJ, Ferguson JA, Walt DR. Nat Biotechnol. 2000; 18:91. [PubMed: 10625399]
5. Han M, Gao X, Su JZ, Nie S. Nat Biotechnol. 2001; 19:631. [PubMed: 11433273]
6. Battersby BJ, Lawrie GA, Johnston APR, Trau M. Chem Commun. 2002; 14:1435.
7. Braeckmans K, De Smedt SC, Leblans M, Pauwels R, Demeester J. Nat Rev Drug Discovery. 2002; 1:447.
8. Gao X, Nie S. J Phys Chem B. 2003; 107:11575.
9. Gao X, Nie S. Anal Chem. 2004; 76:2406. [PubMed: 15080756]
10. Smith AM, Dave S, Nie S, True L, Gao X. Expert Rev Mol Diagn. 2006; 6:231. [PubMed: 16512782]
11. Ritter H, Bruhwiler D. J Phys Chem C. 2009; 113:10667.
12. Salmio H, Bruhwiler D. J Phys Chem C. 2007; 111:923.
13. Koole R, van Schooneveld MM, Hilhorst J, de Mello Donegá C, ‘t Hart DC, van Blaaderen A, Vanmaekelbergh D, Meijerink A. Chem Mater. 2008; 20:2503.
14. Graf C, Dembski S, Hofmann A, Rühl E. Langmuir. 2006; 22:5604. [PubMed: 16768483]
15. Graf C, Vossen DLJ, Imhof A, van Blaaderen A. Langmuir. 2003; 19:6693.
16. Hu SH, Liu DM, Tung WL, Liao CF, Chen SY. Adv Func Mater. 2008; 18:2946.
17. Insin N, Tracy JB, Lee H, Zimmer JP, Westervelt RM, Bawendi MG. ACS Nano. 2008; 2:197. [PubMed: 19206619]
18. Chan Y, Zimmer JP, Stroh M, Steckel JS, Jain RK, Bawendi MG. Adv Mater. 2004; 16:2092.
19. Liu YS, Sun Y, Vernier PT, Liang CH, Chong SYC, Gundersen MA. J Phys Chem C. 2007; 111:2872.
20. Gao X, Chan WCW, Nie S. J Biomed Opt. 2002; 7:532. [PubMed: 12421118]
21. Spanhel L, Haase M, Weller H, Henglein A. J Am Chem Soc. 1987; 109:5649.

22. Boldt K, Bruns OT, Gaponik N, Eychmüller A. J Phys Chem B. 2006; 110:1959. [PubMed: 16471768]

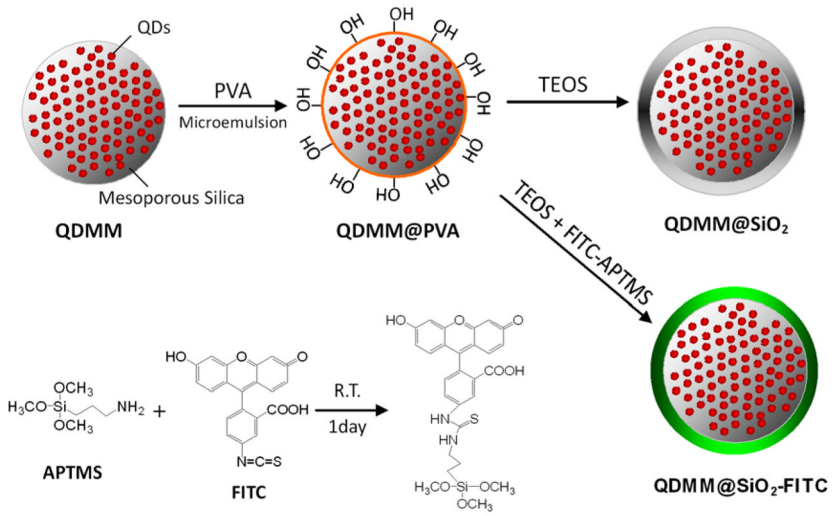


**Figure 1.**

Schematic illustration of key steps involved in silica encapsulation of QDMMs. Hydrophobic QDMMs are stabilized with PVA before addition of silica precursors. For direct visualization of the silica shell, fluorescence silane compounds that emit a different color than the embedded QDs can be used. The chemical reaction of labeling APTMS with FITC is show on the bottom left.

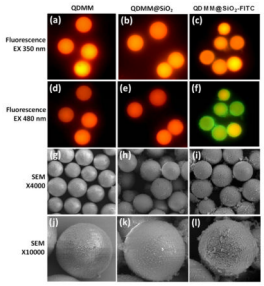


**Figure 2.**

Fluorescence and SEM images of QDMMs before and after silica encapsulation. Fluorescence images of (a-c) QDMMs, QDMM@$SiO_2$, and QDMM@$SiO_2$-FITC excited at 350 nm and (d-f) excited at 480 nm. Under 350 nm excitation, only QD fluorescence (red) were visible; whereas under 480 nm excitation, both QD fluorescence and FITC fluorescence were detected. SEM images at 4,000 and 10,000 magnifications of the of QDMMs (g, j), QDMM@$SiO_2$ (h, k), and QDMM@$SiO_2$-FITC (i, l). After silica shell coating, the surface of microbeads became slightly uneven and granular.

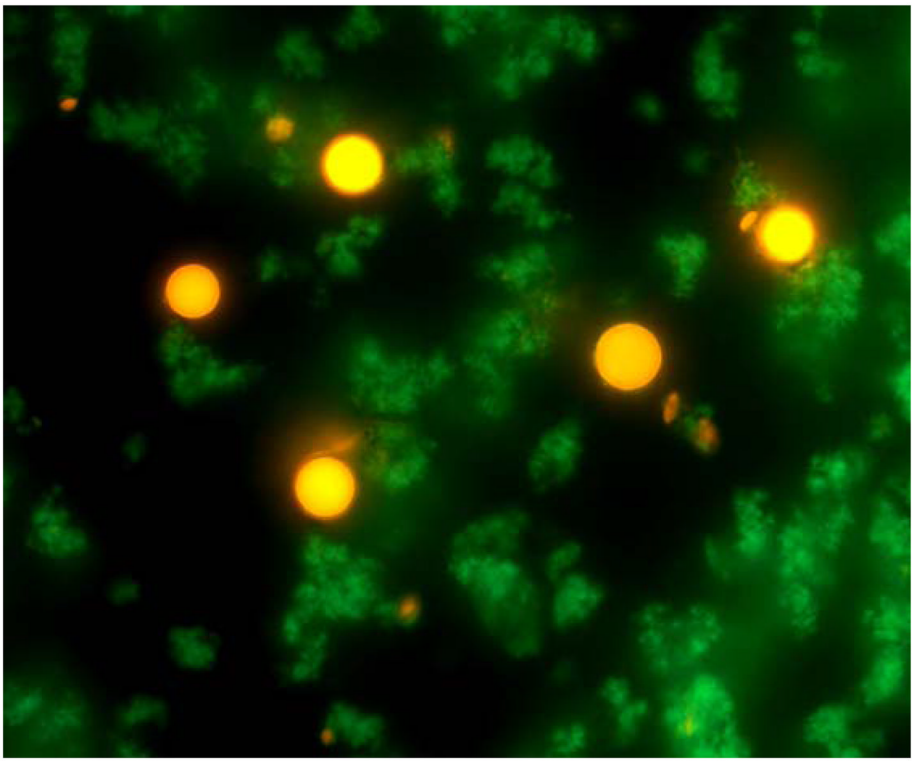

**Figure 3.**
Without the microemulsion process, silane compounds did not nucleate on the surface of QDMMs and further develop into silica shells. They self-nucleated and condensed into irregularly shaped aggregates (green aggregates in the background).

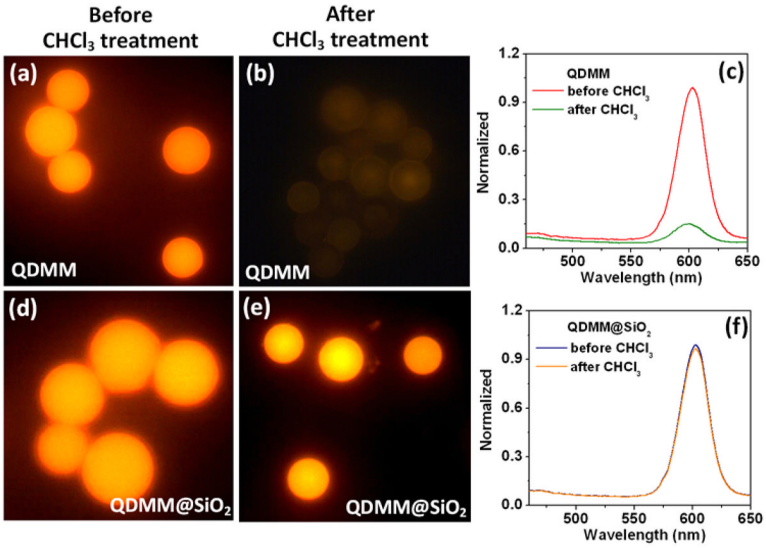


**Figure 4.**

Fluorescence imaging of solvent induced nanoparticle leaching. Fluorescence microscopy images of QDMMs (a, b) and QDMM@$SiO_2$ (d, e) before and after sonication for 2 minute in chloroform, respectively. QDs in the uncoated QDMMs rapidly diffused out but not in the QDMM@$SiO_2$ case. (c, f) Quantitative spectroscopy results show that the fluorescence intensity of uncoated QDMMs decreased by 85%. In contrast, after silica coating, QDMM@$SiO_2$ fluorescence drop was less than 2% after chloroform treatment.

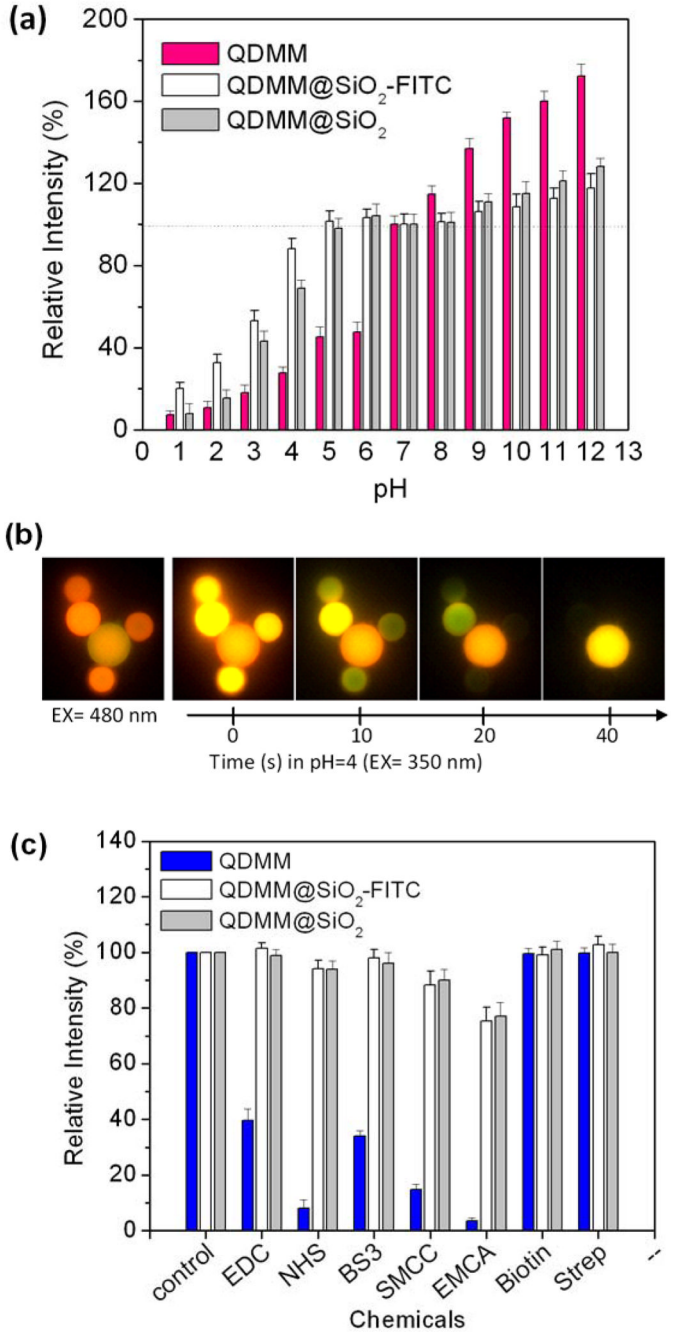


**Figure 5.**

Stability comparison of QDMMs before and after silica encapsulation. (a) Relative fluorescence intensity of QDMM, QDMM@$SiO_2$ and QDMM@$SiO_2$-FITC in solutions with pH ranging from 1 to 12. Between pH 5 and 8, the fluorescence fluctuation of QDMM@$SiO_2$ and QDMM@$SiO_2$-FITC was below the measurement standard deviations; whereas at pH 5, the fluorescence of uncoated QDMMs decreased by more than 50%. Under strongly acidic or basic conditions, the fluorescence of QDMM@$SiO_2$ fluctuated at a lesser degree compared with QDMMs. (b) In situ microscopy imaging of QDMM and QDMM@$SiO_2$-FITC at pH 4. The QDMMs were quenched significantly faster than the silica encapsulated microbeads. The two sets of microbeads were distinguishable when

excited at 480 nm due to the FITC emission. (c) Chemical stability of QDMM, QDMM@$SiO_2$ and QDMM@$SiO_2$-FITC when treated with common bioconjugation reagents.